Under-deposit corrosion

<div style="float:right">**15**</div>

Bruce Brown [1] and Jeremy Moloney [2]
[1]Ohio University, Athens, OH, United States; [2]Nalco Champion, An Ecolab Company, Sugar Land, TX, United States

15.1   Introduction

Produced fluids from many oil and gas wells have been known to carry silt, sand, and solids from the geologic reservoir, which can be left behind as deposits along the interior of a production or transmission pipeline. These deposits become a diffusion barrier between the produced fluids and the interior pipe wall, which results in the water chemistry near the steel surface to differ from that of the bulk fluids. Observations from laboratory studies and field cases have shown that these deposits influence corrosion mechanisms and lead to a localized corrosion called under-deposit corrosion (UDC). Often found at low-flow areas inside pipelines, UDC is a very aggressive form of corrosion that occurs when suspended solids and precipitated phases are given the opportunity to settle to the bottom of the pipeline. The three general categories of deposits include inorganic deposits, such as sand, clay, and corrosion products; organic deposits, such as asphaltenes and wax; and "schmoo," which is a mixture of organic and inorganic deposits [1].

Depending upon the environmental attributes and the type of deposits, different corrosion mechanisms can be applied to explain UDC. The main observation from laboratory studies [2−7] has been the large increase in electrical potential difference that occurs between a metal electrode under a sand deposit and a bare metal electrode, both in the same solution, when an inhibitor was added. The bare metal electrode would increase to a more positive potential because of the reduction in both anodic and cathodic reactions, whereas the potential of the UDC electrode might not be affected at all as a result of the sand acting as a diffusion barrier toward the corrosion inhibitor. When these two metal electrodes were connected together, the UDC electrode experienced a strong anodic polarization and, thus, galvanic corrosion. Other laboratory studies that focused on a single UDC electrode [8−14] found that the influence of a deposit on corrosion and mitigation mechanisms was to create a mass transfer barrier that limited the transfer of species (ions, inhibitors, and biocides) to and from the metal surface. Experiments have also shown deposits to provide additional surface area, which causes parasitic adsorption of inhibitors and biocides, and in turn their effectiveness is reduced. The review of research observations provided in this chapter on UDC contains information on the effect of deposits on the surface area for localized corrosion, types of deposit materials, experimental methodologies, mitigation methods for UDC, and gaps in the current knowledge that require future research.

15.2   UDC mechanisms related to the deposit

Solids are often carried by the fluid flow from the reservoir and can accumulate in an operating pipeline to become a deposit when the energy of the flow is not high enough to keep them suspended or moving. These deposits are understood to contain a mixture of water, hydrocarbons, microorganisms, and inorganic compounds along with corrosion products and scales, which, of course, differ from field to field and almost certainly differ down the same pipeline as water chemistry conditions change with temperature and pressure. It is also understood that the corrosion mechanisms are influenced by whether the deposit is inert or conductive. In this section, some of the components that make up the deposits and how each will influence corrosion, along with a calculation of the cathode to anode area ratio that can be developed in relation to the depth of the deposit, are reviewed.

15.2.1   Inert deposits

Most commercial oil and gas reservoirs occur in sedimentary rock deposits because of their characteristic permeability and porosity. Sedimentary rocks form in the Earth's crust through a sequence of physical, chemical, and biological processes. Common sedimentary minerals include silicates, carbonates, clay, and iron. Silicates and carbonates make up most of the rock-forming minerals and are considered insulators with electrical resistivity greater than 10^9 ohm·m. Sand, silt, and clay are classified by grain size and composition. Sand ranges in diameter from 2 to 0.063 mm, whereas silt ranges in diameter from 0.063 to 0.002 mm, and clay is defined as less than 0.002 mm in diameter. Both sand and silt are mainly composed of SiO_2-rich particles, whereas clay is composed mainly of aluminosilicates with a sheet structure [15]. Although some reservoirs have an inherent problem with the production of solids, high rates of production from a reservoir or a stimulation treatment to increase production from an existing well may also cause the migration of formation sand, silt, and clay through the production string into the pipeline.

   The presence of non-conductive or inert deposits, such as sand, silt, and certain scales, on the pipe wall can act as a diffusion barrier to limit the mass transfer of corrosive species, inhibitors, biocides, or other oilfield chemicals from the bulk solution to the metal surface. When this is the only mechanism involved in corrosion, this diffusion barrier generally retards the corrosion under the body of the inert bed. To prove this mechanism, Huang et al. [8] tested clean inert solid deposits with different particle sizes (SiO_2 powder, glass beads, and sand) to determine the effect of the deposited solids on the fundamental mechanisms of CO_2 corrosion. The specially designed metal specimen holder used in that study is shown in Fig. 15.1. The three layers of the holder were used to (1) isolate the electrical connections from the solution, (2) support a removable metal specimen so only the top of the specimen was exposed to the environment, and (3) define the thickness of the sand bed. Using this type of specimen holder to generate a reproducible 5-mm depth for each inert solid deposit, a linear relationship between the deposit porosity and the average CO_2 corrosion rate of an X65 steel in 24-h experiments was obtained (Fig. 15.2).
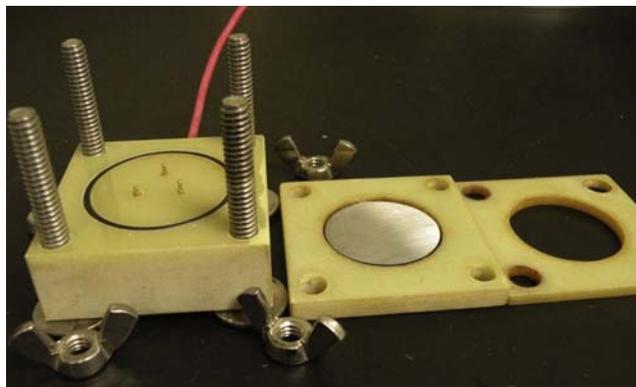
Figure 15.1 Specimen holder: (a) base, with three gold contacts to connect the steel specimen and wire for electrochemical measurements; (b) steel specimen holder; (c) sand holder, machined to the desired depth of the sand deposit [16].

This linear relationship between the deposit porosity and corrosion rate [16] was an indication that both anodic and cathodic reactions were significantly retarded underneath the deposited inert solids. As ferrous ions are released from the metal surface under a deposit, their concentration is much greater near the metal surface because of the slow flux through the low porosity of the sand bed to the bulk solution. The increase in ferrous ion concentration increases the pH and saturation value near the metal
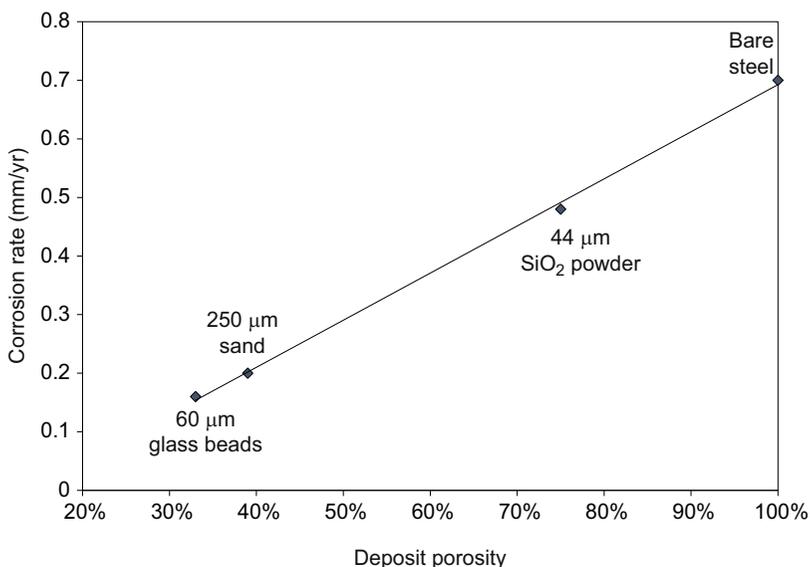
Figure 15.2 Deposit porosity and CO_2 corrosion rate relationship (pH 5, 25°C (77°F), 1 bar (14.5 psi) pCO_2, deposit depth 5 mm, 24 h) [8].

surface, leading to near surface precipitation. This was proved by Huang et al. [8], who found that the pH under the deposit was consistently near pH 6 independent of temperature (25 and 80°C or 77 and 176°F, respectively), type of deposit (SiO_2, sand), and bulk solution pH (pH 4, 5, and 6). When an inert deposit was used to fully cover the steel specimen, these types of deposits were not found to cause localized corrosion but to have consistently low CO_2 corrosion rates under the deposits for all the conditions tested. As the corrosion products within the inert deposit increase with time, corrosion was limited by blocking sites on the surface where metal loss or cathodic reactions might occur. The sand bed literally starved the reaction of the fuel that it needs to continue.

15.2.2   Conductive deposits

Iron sulfides are probably the most encountered semiconductive deposit types in oil and gas production and transmission pipelines. Numerous iron sulfides can exist, the nature of which is dependent on the environment and operating parameters. Rickard and Luther [17] provide a comprehensive review of the chemistry of iron sulfides, including their semiconductive properties. A semiconductor is a crystalline or amorphous solid with an electrical resistance (ER) much larger than metals, but with lower resistance than an insulator, that increases in electrical conductivity with an increase in temperature. Electrical resistivity is the inverse of the material's electrical conductivity. Electrical resistivity has the greatest variation of any materials' physical property from metals as low as 10^{-7} ohm·m to insulators at approximately 10^{20} ohm·m, where semiconductors range from having insulator properties (10^6 ohm·m) to being conductive (10^{-5} ohm·m). Iron sulfides, such as pyrrhotite and pyrite, have been measured to have a resistivity between 10^{-5} and 1 ohm·m, which is in the higher range of conductive properties for a semiconductor [18,19].

Research on the effect of iron sulfides on corrosion of mild steel has shown their influence on anodic and cathodic reactions [20,21] and their influence on accelerating corrosion [11,22]. In a UDC study on X65 steel, Menendez et al. [11] used five different types of iron sulfide deposits obtained from various sources, which were characterized with respect to their particle size, crystalline structure, and surface composition using particle size analysis, X-ray diffraction, and X-ray photoelectron spectroscopy. Corrosion studies were conducted at 65°C with partial pressures of 370 bar (5.4 ksi) pH_2S and 710 bar (10.3 ksi) pCO_2. In 100-h autoclave corrosion testing, mass loss specimens fully covered with one of the specific iron sulfide deposits show that the mackinawite-type deposit facilitated the most corrosion. X65 specimens covered with two synthesized batches of mackinawite had general corrosion rates of up to 4 mm/year, whereas those covered with mackinawite synthesized with excess Na_2S exhibited the highest general corrosion rate of 6 mm/year. However, specimens covered with two commercially acquired iron sulfide powders only had general corrosion rates of 0.2 mm/year. When specimens in an autoclave were exposed to similar conditions with 48,500 ppm Fe^{2+} in solution to induce mackinawite precipitation over 168 h, the general corrosion rate was only 0.6 mm/year, but pitting corrosion ranging from 300 to 500 μm in depth (greater than 2500 mm/year) proved that the

precipitated mackinawite facilitated localized attack. The localized corrosion morphology produced in the mackinawite precipitation experiments was considered to have good agreement with UDC attack observed in the field. Jing et al. [22] also found localized corrosion was initiated once a sufficient amount of mackinawite corrosion product had formed and was transformed into greigite and/or pyrrhotite. The initiation of localized corrosion was thought to be due to the galvanic effect exaggerated by the differences in electrical conductivity of the different iron sulfides.

One specific study on iron sulfide UDC focused on evaluating the galvanic corrosion through the use of a specialized probe with an actual field sludge deposit in a CO_2/H_2S environment. Alanazi et al. [9] conducted weight loss and electrochemical corrosion tests using a coupled multielectrode array system (CMAS) that contained 25 flush-mounted carbon steel rods (UNS G10180) with an active surface area of 0.45 cm^2 and a 1.5-cm-thick sludge deposit. Analysis of the sludge deposit shows that it was made up of 85 wt% $CaCO_3$, 8 wt% pyrite, and 3 wt% mackinawite with smaller amounts of other inert species. The CMAS was coupled to a carbon steel rod (UNS G10180) with an approximate surface area of 26 cm^2, which was in the bulk solution. The gas mixture used was 0.1 mol% H_2S and 0.39 mol% CO_2, with the balance of gas being nitrogen at a total pressure of 1 bar (14.5 psi) and temperature of 48°C (118°F). Electrochemical and galvanic corrosion testing conducted with the CMAS measured average galvanic corrosion rates of 30 mm/year underneath the sludge deposit when coupled with the electrode not under the deposit. Under the same environmental conditions, the 2.54-cm-diameter weight loss specimens without deposit had general corrosion rates less than 1 mm/year over a 24-h experiment time. The mackinawite in the field sludge was believed to be the cause of the very high localized corrosion rates observed for the multielectrodes. This was expected because the mackinawite is conductive, but the weight loss specimens were also a reminder that the high localized corrosion required a large cathode external to the deposit to drive the high corrosion rates.

15.2.3 Effect of deposit on surface area in inhibited pipelines

In a pipeline, sand and solids tend to collect along the bottom of the cylindrical surface as a result of gravity, leaving a much greater metal surface area within the pipeline that is not under the sand bed. For example, an inhibited water injection line with a full pipe flow containing a sand bed with a depth that is 1% of the pipe diameter can have almost 15 times more cathodic area from the pipe walls than the anodic area under the sand bed. Fig. 15.3 shows the relationship between the depth of an inert sand bed (% depth ratio) in a pipeline and the ratio between the surface area of the pipeline above and below a deposit (ratio of cathode area to anode area) in an inhibited full-pipe flow.

Many laboratory experiments have been designed to evaluate an inhibitor's performance in the presence of an inert sand deposit. These experiments have been designed to study the effectiveness of an inhibitor through a sand bed and have used cathode to anode area ratios of 4:1 or smaller. From Fig. 15.3, it can be seen that a 10% sand bed depth ratio (i.e., 1 cm sand depth in a 10.1-cm-diameter pipeline) is almost equivalent to a 4:1 cathode to anode ratio in an inhibited pipeline.
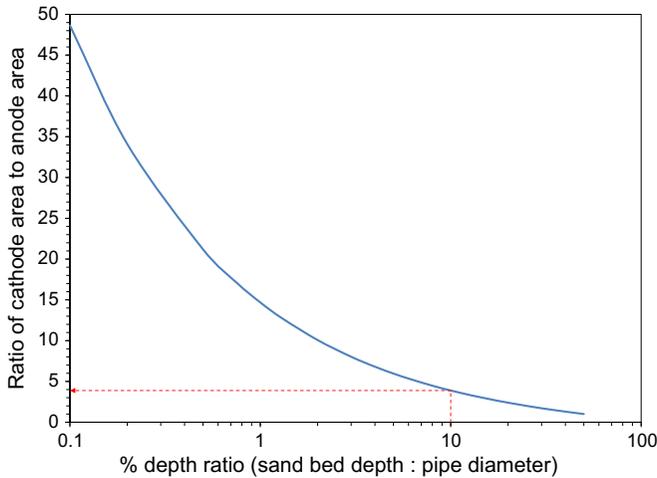
Figure 15.3 Ratio of cathode to anode based on sand depth.

15.3   Research methodologies

There are many different methods that have been used to study UDC in controlled lab-oratory conditions. Testing methods used by various researchers have been developed based on postulates for UDC mechanisms from failure analysis and laboratory studies, so research in this area has varied widely. Studies have focused on the mechanisms of solid deposition, the chemical makeup of the solid deposit, mechanisms of diffusion through the solid deposit, and the galvanic effect, which can be caused by the presence of both a solid deposit and the ever necessary corrosion inhibitor. The fact that UDC is a form of localized corrosion is even viewed differently by different researchers. If there is a higher general corrosion rate under the entire deposit as compared with the remaining pipe walls in an inhibited system, then the localized corrosion area of metal loss is under the entire sand bed. But most of the discussion in the literature has focused on finding deeper pitting corrosion that occurs within the area underneath the sand bed. Experiments to uncover corrosion mechanisms related to UDC have looked at the lack of inhibitor reaching the metal surface under the deposit, the corro-sion experienced by a single metal specimen under the sand deposit, and the effect of galvanic corrosion when using multiple metal specimens in the same experiment (one metal specimen with a deposit coupled to another metal specimen without a deposit in the same solution).

As with any research topic, UDC has been studied with many different viewpoints because of the various possible compositions of the deposit and the method in which it was deposited. In experiments related to diffusion through solids, many have sug-gested parasitic consumption of inhibitor on the large surface area of the sand particles as the reason for loss of inhibition and the occurrence of localized corrosion [4,13,14,23]. In experiments using electrochemical measurements of coupled metal

specimen to characterize the UDC phenomena, it was understood that the presence of certain inhibitors in association with the characteristics of the deposit would induce a galvanic cell with the anodic part being the small area under the sand bed and the cathodic part being the much larger surface area of the surrounding pipeline [3−7,9,13,16,23]. In experiments using an uncoupled metal specimen to understand the role of the deposit material in UDC, it was understood that the depth of the deposit mainly creates a diffusion barrier that should cause widespread corrosion underneath an inert sand bed, but small areas of localized corrosion were found that required more explanation [16,24]. This led to experiments with single sand grains spread out on a single corrosion specimen in the presence of a corrosion inhibitor, which created a methodology for repeatable pit initiation in the presence of a corrosion inhibitor [24,25]. It also changed the viewpoint that parasitic consumption of the inhibitor was the main cause of the observed isolated localized corrosion under a deposit. The link between the coupled metal specimen experiments with only one specimen under a deposit and the single specimen with a partial sand coverage is the galvanic effect that occurred in the presence of an inhibitor. This shows the real need to understand how the mechanisms related to this galvanic effect could be influenced by the inhibitors used to mitigate UDC.

The examples of test methodologies in the following discussion are representative of what is found in the literature. Most techniques have been developed by one set of researchers and slightly tweaked by others to learn something new or to relate to their individual project goal. The one procedure in common with all techniques is that they all involve time for precorrosion before the inhibitor is added.

15.3.1   Parasitic loss of the inhibitor to the solid deposit

Because most inhibitors are surfactants, the first assumption is that an increased surface area caused by the addition of sand will cause a parasitic loss of the inhibitor to the liquid/solid interface. Two types of experiments have been conducted without the sand or deposit material coming into contact with the corroding sample to determine if parasitic loss is a factor for the specific inhibitor being used.

A basic bubble test method [12] has been used to assess if the presence of solids affects the efficiency of the tested inhibitor(s). The sand did not come in contact with the metal being tested but was dropped into the glass cell with the metal to increase the surface area for inhibitor adsorption. An experiment with the sand present in the glass cell would be compared with an experiment with the same exact environmental conditions without the sand. If a higher corrosion rate occurred repeatedly when sand was present in the glass cell, then parasitic loss of the inhibitor was attributed for the difference.

The second method was to use a two-stage test involving column adsorption and then a corrosion inhibition test [13,14]. These experiments used a prescreening column to determine the adsorption and penetration of each corrosion inhibitor on a solid (ideal or field specimen), then used the same inhibitor in a separate corrosion experiment. The corrosion experiment was carried out under selected test conditions using an electrochemically measured specimen with a deposited solid and an electrochemical probe

with no deposit for comparison. Good correlation was observed between low adsorption in the column tests and acceptable performance in the corrosion experiments.

15.3.2   Experiments on coupled specimen

The galvanic effect for coupled specimen, observed in UDC experiments for two metal specimens in the same solution with one under the deposit, has shown this mechanism to be the dominant driving force for localized UDC. The two methodologies shown in the following sections greatly increase the difficulty level for experimental preparations and procedures but have been used to monitor localized corrosion during an experiment through the use of an external potentiostat or zero resistance ammeter (ZRA).

15.3.2.1   Inert deposit test methods

Many researchers have found that there is a large difference in the electrode potential between a sand-covered mild steel specimen and a noncovered mild steel specimen when both are exposed to a corrosion inhibitor. When these two specimens are coupled together, using similar anode to cathode surface area ratios that might exist in an inhibited pipeline, the galvanic current between them leads to localized corrosion under the deposit.

The sand deposit test method [4] has been used to investigate environments where sand or mineral scale deposition was possible. These experiments were conducted in a 3-L glass cell with a test apparatus designed so that prepared sand could easily be added during the experiment on top of the API 5L X65 specimens. Three metal specimens were molded into a flat epoxy square, such that the two 1 cm^2 surface area specimens were next to each other and parallel to the one large 4 cm^2 surface area specimen. The square epoxy mold was mounted in the test apparatus at approximately 45 degrees angle so that the bottom two specimens would be covered by about 5 mm sand after a 2-h precorrosion. Only one of the small specimens was galvanically coupled to the non-sand-covered specimen creating a 4:1 cathode to anode surface area ratio when inhibitor was present. This design provided direct proof of the effect of sand on inhibitor performance and the effect of inhibitor on UDC. The key observation in studies with this apparatus proved the effect of inhibitor addition on the galvanic couple between a sand-covered specimen and a bare specimen that would polarize the sand-covered specimen anodically, leading to localized attack.

Testing by Pedersen et al. [2] found an increase in the open circuit potential (OCP) of an individual bulk solution specimen without sand as compared with the OCP of an individual specimen underneath a 5-mm sand deposit. Their experiments used two specimens fully covered in sand (FS1 and FS2), each of 1 cm^2 surface area, along with one specimen with no sand (NS) of 4 cm^2 in area. When NS and FS1 were coupled together, the coupled potential would be closer to the OCP for NS because of the 4:1 cathode to anode ratio. The change in OCP for FS1 was believed to be the driving force for galvanic corrosion. This experimental technique provided an

evaluation methodology for determining the effectiveness of specific inhibitors toward localized corrosion inhibition in UDC and should be considered beneficial for inhibitor comparison studies. For this methodology, factors identified during inhibitor testing on UDC conditions that increase the susceptibility to localized corrosion would include the degree of anodic polarization of a single specimen, the effect of underdosage of the inhibitor, the effect of degradation of the inhibitor with time at higher temperatures, and the effect of corrosion product layer formation. In these studies [2], testing of two inhibitors under similar conditions proved that inhibitor chemistry played a role in the mitigation efficiency of UDC, with an imidazoline salt showing better efficiency than an alkyl amino acid.

A series of experiments by Barker et al. [3], utilizing the electrode configuration in Fig. 15.4, considered the influence of inhibitor components, which included imidazoline, phosphate ester, sodium thiosulfate, and 2-mercaptoethanol, with results indicating the two sulfur-containing compounds had the highest mitigation efficiencies toward UDC general corrosion. Each inhibitor component chemical was tested at 45 ppm, equivalent to a 150-ppm inhibitor package with 30% active chemical. A test duration of 20 h was used for the comparison but was not considered long enough to develop localized corrosion on the individual 1 cm^2 surface area specimens underneath the sand bed. The phosphate ester inhibitor had the highest mitigation efficiency on the bulk solution specimen in the presence of sand, whereas it had the lowest mitigation efficiency on UDC; this led to the conclusion that consumption of inhibitor by an excessive sand surface area may not be the initiator for localized corrosion and other factors may be responsible. For each inhibitor component, it was found that the deposition of sand retarded both anodic and cathodic reactions at the steel surface. With the addition of most of the inhibitors, the galvanic current between the UDC electrode and the sand-free electrode was observed to favor anodic dissolution under the deposit. The sodium thiosulfate and the 2-mercaptoethanol were found to decrease the general UDC rates to less than 0.1 mm/year at bulk solution concentrations as low as 5 ppm.
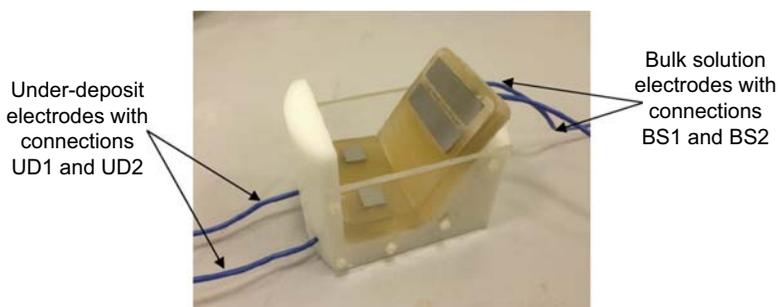
Figure 15.4 Specimen holder having under-deposit working electrodes with a 1 cm^2 area and bulk solution working electrodes with a 4 cm^2 surface area [3].

15.3.2.2 Coupled multielectrode array

A coupled multielectrode array (CMAS) test or wire beam electrode (WBE) method [5−7,10] uses multiple small-diameter wires or pins flush mounted in an inert material that are coupled together externally from the test environment so that the electrode array can be tested as one piece of metal or monitored individually for galvanic corrosion and/or localized corrosion. The cited work have used either a 24-electrode array [5,6,10] or a 100-electrode array [7].

As shown in Fig. 15.5, the 24-electrode array was designed using a polyethyl ethyl ketone (PEEK) casing around the electrodes, which was fitted into a polytetrafluoroethylene cup that would hold 10 mm of an inert deposit. Analysis of the multielectrode array was performed by progressive polishing of the PEEK holder containing the electrodes to physically determine the depth of corrosion that occurred to the nearest 20 μm. Experiments using this device [6] confirmed the addition of an inhibitor polarized a non-sand-covered electrode to a more noble potential with respect to a sand-covered electrode, which accelerated the corrosion rate under the sand deposit. In most of their experiments with industrial inhibitors relevant to oilfield applications, this galvanic corrosion would continue in excess of 30 days.

Hinds and Turnbull [10] used a 24-pin multielectrode probe under two different CO_2/H_2S partial pressure ratios of 5:3 (1.67 bar or 24 psi pCO_2 with 1 bar or 14.5 psi pH_2S) and 100:1 (2 bar or 29 psi pCO_2 with 0.02 bar or 0.29 psi pH_2S) with a 1-cm sand bed with particles of 0.1−0.3 mm diameter in a 10-L autoclave. The precorrosion step was conducted in a CO_2-purged solution by applying an anodic current of 1273 A/m^2 to individual 1-mm-diameter electrodes (UNS G10180) for a defined time before the addition of H_2S to corrode sets of pins to a specific depth (eight at 1 mm, eight at 0.1 mm, and eight uncorroded). Because of this, there was no uninhibited baseline corrosion rate for comparison. After precorrosion, all 24 pins were galvanically coupled to an external carbon steel rod (UNS G10180) with an
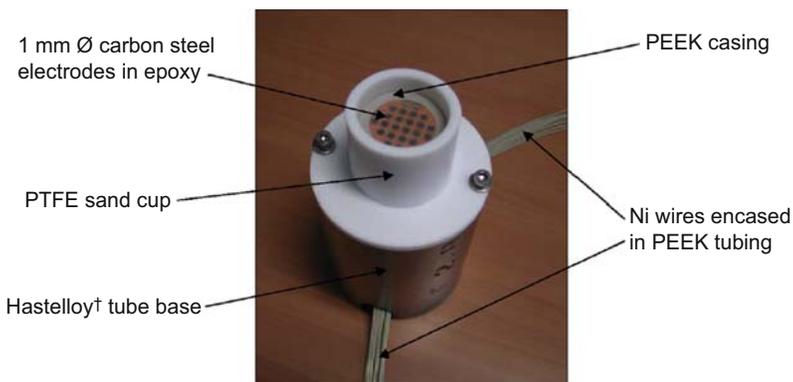
Figure 15.5 Coupled multielectrode array [6]. *PEEK*, polyethyl ethyl ketone; *PTFE*, polytetrafluoroethylene; †, trade name.

Galvanic current distribution
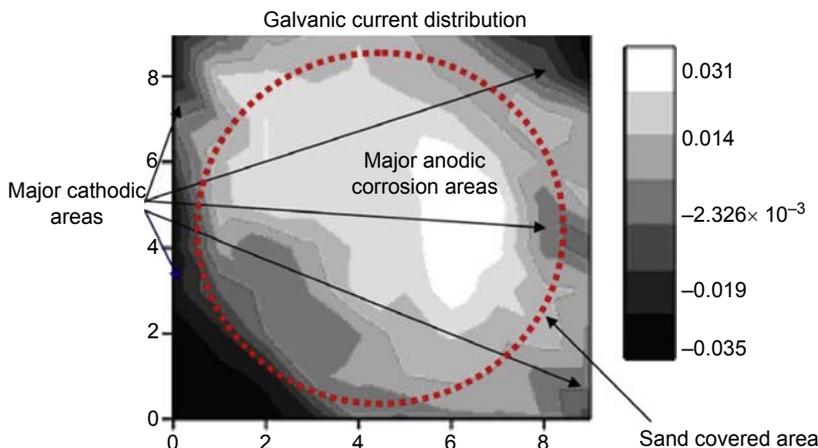
Figure 15.6 Galvanic current distribution map measured using a wire beam electrode exposed to CO_2 under-deposit corrosion conditions with imidazoline-type inhibitor present [7].

approximate surface area of 32 cm^2, which was in the bulk solution, and inhibitor was added. The CO_2/H_2S gas mix was then added and galvanic corrosion rates were monitored until the corrosion rate on most pins was less than 0.1 mm/year. They found that the amount of time for the inhibitor to provide protection through the sand bed was related to the amount of precorrosion as the non-precorroded pins were inhibited within 2 days, the 0.1-mm-depth precorroded pins were inhibited within 4 days, and the 1-mm precorroded pins took 4 days to achieve the desired corrosion rate.

As shown in Fig. 15.6, the 100-electrode WBE array [7] was used to directly measure the galvanic current distribution under the deposit. This typical map was collected in a CO_2-purged solution at 25°C (77°F) after 10 ppm imidazoline inhibitor was added. Notice that the anode areas are located within the ring under the sand deposit, whereas the cathode areas are mainly located where no sand was present. The maximum anodic current measured ranged from 0.022 to 0.034 mA/cm^2 in the central areas of the deposit.

15.3.3 Experiments on an individual specimen

Experiments using a single corroding specimen under a deposit are focused on the deposit's direct effect on the basic corrosion mechanisms associated with the deposit and/or the inhibitors' ability to diffuse through the deposit or under the individual sand grains to the metal surface. From the literature, as well as the research previously reviewed in this chapter, it appears as though there is a general consensus that a stagnant deposit acts as a diffusion barrier that slows down the transfer of corrosive species, inhibitors, and/or biocides to the metal surface while also slowing down the transport of corrosion products away from the metal surface. There is also strong evidence that the mechanism of galvanic corrosion occurs between deposit covered and

noncovered areas in the presence of specific inhibitors, even when the metal surface has a partial or minimal coverage by an inert deposit.

15.3.3.1 Full coverage deposit

A lot of experimentation has been carried out using a single specimen underneath a deposit to access the effect of the deposit on corrosion and corrosion mitigation. This type of testing should be completed as a first step to develop the foundation of information used to understand more complex corrosion mechanisms or could be used in more complex systems to gain insight on specific issues. The first example helps to build the foundation of information through repeatable experiments in a cup-style specimen holder to provide a consistent sand bed depth for electrochemical or weight loss studies in an autoclave. The second example used specially designed equipment to experimentally compare the in situ inhibited corrosion rate for a specimen with an iron sulfide corrosion product layer with a similar specimen with a deposit of iron sulfide deposited as a precipitate from the bulk solution to understand the effect of each on corrosion mitigation. The third example delivers a broader scope of the more foundational information by changing the environmental parameters of temperature, sand thickness, and inhibitor dosage to understand the effect of each on UDC and the mitigation of UDC. The different test methods discussed later show an increase in the desire to provide experimental methodologies to uncover corrosion mechanisms related to UDC.

The UDC autoclave method [13] is an extension of a regular inhibitor autoclave test with a special specimen holder that had a 1-cm raised edge to hold nonconductive solids on top of a concentric ring—type three electrode and a regular three-finger linear polarization resistance (LPR) probe to measure general corrosion. After the precorrosion step without the solid deposit, the specimens were removed from the autoclave, rinsed with ethanol, and quickly dried with nitrogen gas. The cup was filled with deoxygenated prepared sand and the autoclave put back together for the remainder of the experiment. Reported tests included four inhibitors plus a blank test with no inhibitor and no deposit. Test times ranged from 6 to 30 days, with most at 25 days. It was suggested that an inhibitor must provide good mitigation efficiency for a non-deposit-covered specimen before it should be tested with a deposit, but that does not always mean the inhibitor will perform well with a sand deposit present. If H_2S and/or iron sulfide deposits are present, then the electrochemical portion cannot be used but can be exchanged for a weight loss specimen (weight loss and microscopic examination for pitting). To overcome this limitation and facilitate electrochemical monitoring under FeS, a setup and approach for monitoring the corrosion rate under iron sulfide deposits has been proposed [26]. In this methodology, the UDC working electrode containing the FeS and the reference and counterelectrodes were separated to avoid bridging problems. It was highlighted that close attention needs to be paid to optimizing the potential scan rate of the LPR measurement to overcome shortcomings in overestimating the corrosion rate, which was attributed to the large interfacial capacitance induced by the presence of the iron sulfide. This optimized approach showed that the electrochemical corrosion rates measured under FeS deposits correlated quite well to the volume loss corrosion rates.

An iron sulfide test method for inhibited systems [27] was developed to perform ER, LPR, and weight loss in an H_2S/CO_2 environment where the FeS deposit could be developed by injection of ferrous chloride or by in situ corrosion of the specimen. This experimental setup was designed to assess the effect of the iron sulfide deposit (mackinawite) on H_2S/CO_2 corrosion and corrosion mitigation on a square ER probe in experiments that could include the use of a hydrocarbon phase. Results found that a carbon steel with an in situ precipitated iron sulfide deposit had around four times higher corrosion rate than the carbon steel probe suspended in the same inhibited solution.

In addition to the physical methodologies used in testing UDC, the environmental parameters also need focused research. In one study designed at assessing such factors [23], multiple experiments designed to determine the critical parameters that affect galvanic corrosion and the effect of inhibition on UDC were conducted. The experiments within the investigation covered temperatures from 25 to 70°C (77−158°F), sand thickness from 1 to 10 mm, and inhibitor dosage from 50 to 200 ppm using a 1-L glass cell with a CO_2 sparged 10 wt% NaCl solution. The apparatus (Fig. 15.7) was based on a typical bubble cell arrangement using a cylindrical UNS G10180 working electrode in solution (solution electrode) along with a saturated silver−silver chloride reference electrode (REF) and a stainless steel UNS S31600 counterelectrode (AUX). For under-deposit measurement, a UNS G10180 working electrode was flush mounted in epoxy with a glass tube to ensure a reproducible sand thickness (UDC electrode) and was coupled to the solution electrode to create a specimen area ratio of 17:1
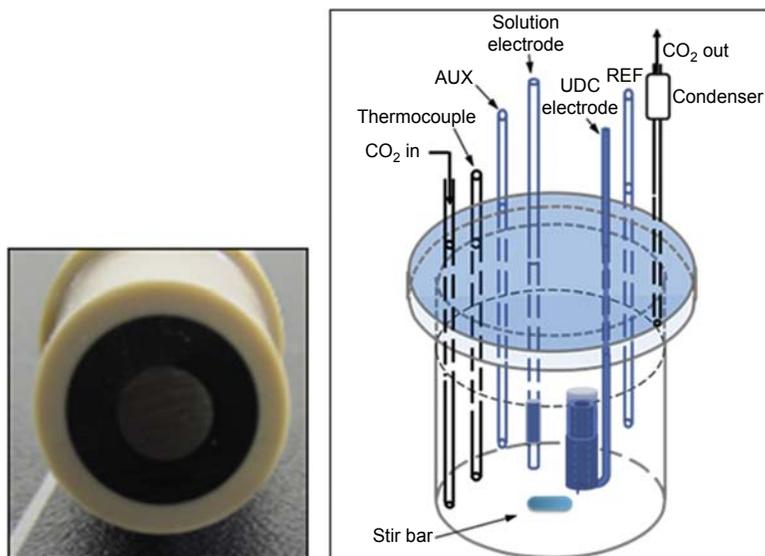
Figure 15.7 (a) Metal electrode sealed in polyethyl ethyl ketone sleeve with epoxy. (b) Under-deposit corrosion (UDC) testing setup [23].

(solution electrode: UDC electrode). The four-electrode system was coupled via a ZRA to observe the galvanic corrosion taking place.

The six major conclusions from this study shown in the following list agree with all experimental results previously reviewed while giving insights on having a thicker sand deposit, an elevated temperature, or a higher concentration of inhibitor.

1. With no inhibitor present, the solution electrode acted as the anode while the sand-covered electrode acted as the cathode.
2. Addition of inhibitor quickly reduced the corrosion rate of the solution electrode, whereas the UDC electrode experienced a strong anodic polarization.
3. As a result of this galvanic coupling, the UDC rate dramatically increased and was measured as high as 17.3 mm/year.
4. A thicker sand deposit was observed to slow the diffusion of inhibitor to the metal surface underneath, which resulted in a higher galvanic current density peak and an ultimately higher corrosion rate under the sand.
5. An increase in the inhibitor concentration also increased the galvanic current over a short period of time, but the higher concentrations did penetrate the sand bed and caused a decay in UDC.
6. Although an increase in temperature caused the solution electrode corrosion rate to increase by 150%, the UDC corrosion rate increased only by 40%.

15.3.3.2   Partial coverage deposit

In tests with a single specimen under a deposit, Huang et al. [24] reviewed the performance of an imidazoline-type inhibitor to understand mechanisms related to localized corrosion. The specimen holder (Fig. 15.1) was placed in a 2-L glass cell (Fig. 15.8) with deaerated brine for precorrosion, before the inert deposit would be transferred from a previously deaerated solution to the area on top of the specimen sand holder. These experiments were conducted over a period of 2−4 days.

They reported that general depletion of the surfactant inhibitor by adsorption on the silica sand surface and slow diffusion through the porous sand layer were not considered critical factors leading to localized corrosion, but proposed a new mechanism that the cause for localized corrosion was related to the inability of the corrosion inhibitor to protect the steel surface in the crevices immediately underneath each sand particle. By testing a single metal specimen with partial sand coverage, it was observed that the lack of inhibition under a single sand particle leads to the formation of a galvanic cell where the small area under the sand particle became anodic while the larger inhibited area around the particle was the cathode. In comparison with the previous surface area ratios discussed, an individual 250-µm sand particle only required a 1-mm-diameter area around it to have a 15:1 cathode to anode area ratio.

The partial coverage sand bed methodology developed by Huang et al. [24] was used as a repeatable procedure in the experimental comparison of mono- to di-nonylphenol phosphate ester (PE) ratios by Brown et al. [25]. This series of experiments was the first formal attempt to observe the effects of specific chemical components of an inhibitor package on UDC. In experiments lasting 28 days, non-ylphenol PEs were tested at varying mono- to di-PE ratios of 90:10, 70:30, and

1. Reference electrode.
2. Luggin capillary.
3. Platinum counter electrode.
4. CO_2 gas inlet.
5. Condenser.
6. Thermal probe.
7. pH probe.
8. Specimen holder
9. Heater
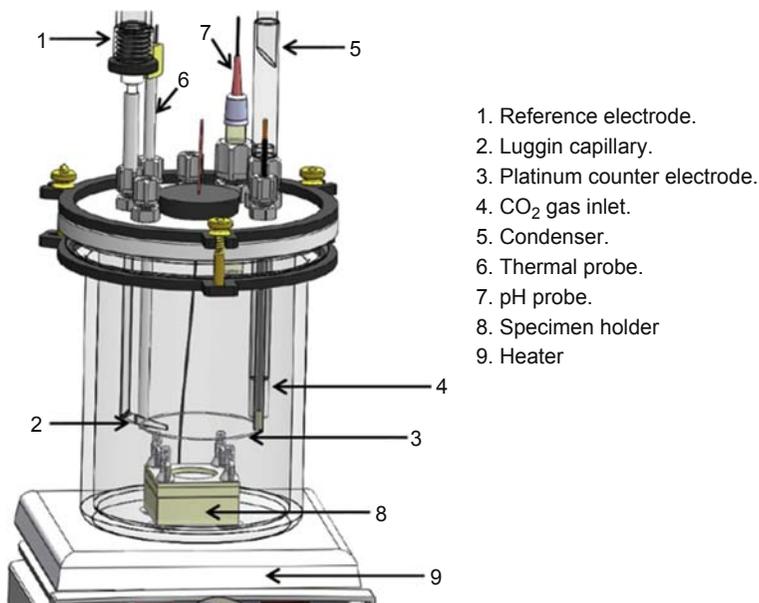
Figure 15.8 Three-electrode glass cell set up for single under-deposit corrosion specimen [16].

50:50. Using an X65 pipeline material partially covered with 250-μm-diameter silica sand particles and exposed to a CO_2 sparged brine at 1 bar (14.5 psi) total pressure and 70°C (158°F), multiple measurement techniques employing electrochemistry, weight loss, and profilometry were used for the comparison. It was found that the presence of 2-mercaptoethanol assisted the nonylphenol PE inhibitors and no localized corrosion was observed. Without the mercaptoethanol, the depth of localized corrosion observed increased with a decrease in the amount of mono-nonylphenol PE in the inhibitor package. This also provided confirmation for the theory of crevice corrosion under each sand particle being the main driving force for localized corrosion.

Multiple small grains of sand or "partial sand coverage" experiments [16] used a few grains of sand on a single metal specimen, which was monitored electrochemically from 25 to 40 days and then analyzed by weight loss and profilometry. The test began with a 2-h precorrosion of the metal specimen, followed by the addition of a few grains of 750-μm sand particles, which had been stored in deoxygenated brine to the 7.9 cm^2 steel surface area. After 24 h the inhibitor was added and the experiment monitored for the remainder of the test time. These experiments showed the inability of a generic imidazoline-type inhibitor to protect the surface directly underneath each sand particle as pit penetration rates of 2.2−3.5 mm/year were found for weight loss specimens having a uniform inhibited corrosion rate of less than 0.1 mm/year. In this type of experiment, the inhibitor can be added before the sand or the sand particles can be moved during the experiment to observe how the inhibitor works with partially stable or moving deposits.

15.4   Mitigation of UDC

The goal of the experimental methods used by various researchers has been to investigate the mechanisms of UDC, which, in some instances, was used to assist in the determination of the most effectual approach for minimizing the threat of pipeline failures. Many strategies have been reviewed with the goal to eliminate UDC by the most cost-effective means available. Most discussions on the topic of UDC mitigation tend to focus on the chemicals used in controlling corrosion as it is understood that the addition of some types of inhibitors creates galvanic corrosion for the area under the deposit. It should also be recognized that these solids can accumulate in pipelines and in turn can cause increased pressure drops as well as enhanced localized corrosion. Removal of the deposits or defining parameters of pipeline operations to limit their formation along with the addition of chemical inhibition by a predefined inhibitor seems to be the most used option to mitigate the attack from UDC. However, the true goal of diminishing or mitigating the probability for UDC may be achieved by other means in the design phase before installation and beginning operations of the pipeline. As with any process or procedure, the easiest and most efficient method should be explored first. The following list provides some approaches for achieving a cost-effective means for minimizing UDC in both the design phase and the operating phase of a pipeline operation.

Mitigation methods for minimizing UDC [12]:

1. In the Design Phase
   a. Design for high flow rates by selecting optimum equipment size.
   b. Minimize stagnant locations.
   c. Install pigging facilities where stagnant locations cannot be avoided.
   d. Use of corrosion-resistant alloys (CRAs) (selection of a proper CRA depends upon many factors and can increase cost).
   e. Use of internal coatings (currently not considered a technique by itself for long-term corrosion protection because of the probability of holidays, delamination, or deterioration; there are also application difficulties for coating existing pipelines with many current coating technologies, although advances are being made in this area).
2. During the Operating Phase
   a. Mechanical removal of debris by pigging (brush pigging with a batch inhibitor treatment).
   b. Chemical treatment with appropriate corrosion inhibitor chemistry and dosage determined through laboratory testing and field trials. Corrosion inhibitors may be added as slugs of concentrated chemicals or through continuous application while other "cleaning" chemicals and surfactants may be used to suspend particles in the liquid phase along with increasing the velocity of produced fluids to aid in transporting the loose solid debris.

In most instances, because the larger capital expenditures for the use of CRAs and coatings may make them less likely to be used, engineers must rely on the two main mitigation strategies during operations: mechanical removal and/or chemical treatments. The following sections provide more information on these topics.

15.4.1 Mechanical removal of deposits (minimum velocities, pigging)

Mechanical removal of deposits starts with designing for higher flow rates in the operating pipeline. A correlation proposed by Salama to predict sand settling conditions can also be used as a valid approximation for velocities to define sand removal [28].

$$V_m = \left(\frac{V_{sl}}{V_m}\right)^{0.53} d^{0.17} \nu^{0.09} \left(\frac{\Delta\rho}{\rho_f}\right)^{0.55} D^{0.47} \tag{15.1}$$

V_m, minimum mixture flow velocity to avoid sand settling, m/s; V_{sl}/V_m, the ratio between the liquid superficial liquid velocity and the mixture velocity at the sand settling conditions (for single phase, this ratio $= 1$); d, particle diameter, m; D, pipe diameter, m; $\Delta\rho$, density difference between particles and the fluid mixture density, kg/m^3; ρ_f, fluid mixture density, kg/m^3; ν, fluid mixture kinematic viscosity, m^2/s.

As the mixture velocity is increased, the critical velocity to begin moving the sand from the sand bed to create a scouring flow or moving dunes is a more complicated process than the reverse process to create the sand bed [28].

For small amounts of sand accumulated in the pipeline, removal can be done by increasing the flow rate or by pigging. Computational fluid dynamics have been used to model the effect of near-wall velocity at the pipe floor on solids deposition to understand the influence of flow and pipeline geometry to aid in this decision [29,30]. For larger amounts of accumulated sand in an operating pipeline, removal by pigging can create hazards by having an excessive buildup of sand ahead of the pig, which could possibly plug the pipeline or damage the process facility by the sudden arrival of a large quantity of sand [28].

15.4.2 Chemical treatment for deposits

The presence of a good performing corrosion inhibitor in a water wet pipeline typically reduces the general corrosion rate by a large amount by adsorption processes at the metal surface. This low corrosion rate is related to a reduction in the anodic and/or cathodic reactions by an effect from the corrosion inhibitor active species on the corroding metal surface. As shown by Dominguez et al. [31], a positive shift in OCP is observed because the corrosion process is under mixed (charge transfer/mass transfer) control and an inhibitor affects only the charge transfer reactions (anodic and cathodic) but not the mass transfer of species to the metal surface. This positive shift in the OCP of a working electrode in a three-electrode system related to the addition of an inhibitor in solution has been observed by others under different environments with different inhibitors [25,32].

When a stagnant deposit is present in an inhibited pipeline, it can be the cause for galvanic corrosion. The deposit acts as a diffusion barrier with a low porosity and high tortuosity for the path from the bulk solution to the pipe wall under the stagnant deposit. This stagnant deposit does not reduce the anodic and cathodic reactions as much as

a good performing inhibitor, but may impede some corrosion inhibitors from reaching the pipe wall. Therefore the smaller area under the deposit does not experience the same effect caused by the reduction in anodic and cathodic reactions as on the larger pipe wall. In laboratory experiments where these areas can be separated, a large potential difference has been observed between the inhibited metal surface in the bulk solution (more positive, cathode) and the noninhibited metal surface under a deposit (more negative, anode). Because a pipeline is one continuous piece of highly conductive metal, there can only be one potential within the general vicinity that is controlled by the larger cathode surface area. The overall potential of the metal adjusts to a mixed potential between the anodic and cathodic reaction-driven potentials, which would be more similar to the cathode potential because of its much larger surface area. The smaller area underneath the deposit compensates for this difference by the transfer of electrons to the cathode. This galvanic corrosion increases dissolution of ferrous ions from the metal surface underneath the deposit to cause high rates of localized corrosion and pitting underneath the deposit as described by the mechanisms discussed and reviewed earlier.

To achieve maximum coverage to the internal pipe wall, added chemicals must be able to diffuse through the deposit to the metal substrate or the deposit must be removed to expose the bare metal surface. Testing has found that 2-mercaptoethanol can assist in mitigating some UDC as it is believed the small size of the molecule (in comparison with other actives such as imidazolines and quaternary ammonium compounds) assists it to penetrate and diffuse more easily through thicker layers and smaller crevices between the sand and the metal of the pipe wall. Some inhibitor package formulations have been developed to aid in the removal of oily sludge-type deposits but rely on flow to maintain a moving slurry of deposit materials in the liquid rather than accumulating along the bottom of the pipe. The aim of these approaches is to keep the pipe wall as clean as possible, which, in turn, allows the maximum amount of inhibitor to adsorb onto the metal surface to not only reduce the overall general corrosion rate but, perhaps more importantly, to minimize the probability of localized corrosion.

When solids, such as sand, clays, corrosion products, and biomass, collect at the bottom of a pipeline, they can become bound together with oil and are known as "schmoo" [33]. This type of deposit is known to create a physical barrier and becomes an ideal environment to grow bacteria leading to microbiologically induced corrosion (MIC). Schmoo was shown to retard the mass transfer of species and corrosion inhibitors to the pipe wall, which aids in the initiation of localized corrosion. Horsup et al. [34] reviewed multiple types of base inhibitor chemicals and tested multiple inhibitor packages on the problem of schmoo removal. They were able to determine two primary mechanisms of emulsification and roll up for the removal of schmoo from laboratory test pipelines and field evaluations, developing a chemical package that was shown to increase flow in a water injection line within 6 weeks after initial dosage. This is a good example of using laboratory testing to better understand the mechanisms of the problem situation and then in turn to utilize this understanding to develop field mitigation solutions. Although it is acknowledged that biofilms (dead or living) can also result in UDC attack, microbiological activity involving this form of UDC has been omitted from consideration in this chapter (see Chapter 8 for MIC).

15.5 Gaps in current research and areas for future study

The use of all components present in UDC field conditions (e.g., sand, iron sulfide, clays, microorganisms, asphaltenes, waxes, hydrocarbon sludges) for a single testing program presents too many variables to be effective and their presence should be limited, or added progressively, in experimental studies to minimize errors in interpretation of results. The focus should be on determining which mechanisms to study under well-controlled conditions that relate to the complex conditions found in the field. Crolet [35] summed up the behavior of corrosion deposits by stating that the conditions of formation, protective properties, and sensitivities to external parameters are extremely different for each case, so that the possible configurations and various working hypotheses to model UDC are too numerous. This infers that studies will still need to be conducted on a case-by-case basis, taking into account the physical characteristics of the deposit (formation, composition, depth, age, etc.), corrosion-related mechanisms (diffusion, precipitation, MIC, etc.), and the associated solution chemistry (water, oil, pH, salt content, etc.) in each case. Much research has been done on these three topics, with numerous companies developing methodologies on how to provide mitigation to their specific problems encountered in the field.

Although various models are available for estimating general corrosion as well as various forms of localized corrosion such as top-of-the-line corrosion, there appears to be limited activity in modeling UDC, which should be a focus for future research. The accumulation of the UDC knowledge base, shared throughout the corrosion community, may be developed not only into a mechanistic model to help predict the extent of UDC, but also as a means to derive mitigation solutions to a much larger base of operators. Furthermore, the knowledge base developed may also aid in the development of future inhibitor formulations and packages that might address the issues found related to the physical characteristics of specific deposits, the corrosion mechanisms, and the solution chemistry in each field.

Continued research needs to be conducted with different surfactant molecules to determine which attributes are valuable to address UDC. Larger inhibitor molecules might be expected to show characteristics of steric hindrance around the small crevices under a sand particle. In the same way that synergistic effects have been seen between molecules in controlling general corrosion, the identification of synergistic combinations of inhibitors for UDC and localized corrosion alleviation would also be advantageous. Such research focus may include studies on the molecular level (atomic force microscopy, molecular modeling, etc.) to better determine and identify types and mixtures of inhibitor molecules tailored for UDC mitigation.

References

[1] J. Vera, D. Daniels, M. Achour, Under deposit corrosion (UDC) in the oil and gas industry: a review of mechanisms, testing and mitigation, Paper no. 1379, in: CORROSION/2012, NACE, Houston, TX, 2012.

[2] A. Pedersen, K. Bilkova, E. Gulbrandsen, R. Nyborg, Testing of CO_2 corrosion inhibitor performance under sand deposits, in: Eurocorr 2007, European Federation of Corrosion, London, U.K., 2007.

[3] R. Barker, B. Pickles, A. Neville, General corrosion of X65 steel under silica sand deposits in CO_2-saturated environments in the presence of corrosion inhibitor components, Paper no. 4215, in: CORROSION/2014, NACE, Houston, TX, 2014.

[4] A. Pedersen, K. Bilkova, E. Gulbrandsen, J. Kvarekvål, CO_2 corrosion inhibitor performance in the presence of solids: test method development, Paper no. 08632, in: CORROSION/2008, NACE, Houston, TX, 2008.

[5] G. Hinds, P. Cooling, S. Zhou, A. Turnbull, Under deposit test method for assessing performance of corrosion inhibitors, in: EUROCORR 2008, 2008. Paper 1254.

[6] G. Hinds, A. Turnbull, Novel multi-electrode test method for evaluating inhibition of under deposit corrosion − Part 1: sweet conditions, Corrosion Journal 66 (4) (April 2010) 046001-1−046001-10.

[7] Y.-J. Tan, Y. Fwu, K. Bhardwaj, Mapping electrochemical evaluation of under-deposit corrosion and its inhibition using the wire beam electrode method, Corrosion Science 53 (2011) 1254−1261.

[8] J. Huang, B. Brown, X. Jiang, B. Kinsella, S. Nesic, Internal CO_2 corrosion of mild steel pipelines under inert solid deposits, Paper no. 379, in: CORROSION/2010, NACE, Houston, TX, 2010.

[9] N.M. Alanazi, A.M. El-Sherik, A.H. Rasheed, S.H. Amar, M.R. Dossary, M.N. Alneemai, Corrosion of pipeline steel X-60 under field-collected sludge deposit in a simulated sour environment, Corrosion Journal 71 (3) (March 2015) 301−315.

[10] G. Hinds, A. Turnbull, Novel multi-electrode test method for evaluating inhibition of under deposit corrosion—Part 2: sour conditions, Corrosion Journal 66 (5) (May 2010) 056002-1−056002-6.

[11] C.M. Menendez, V. Jovancicevic, S. Ramachandran, M. Morton, D. Stegmann, Assessment of corrosion under iron sulfide deposits and CO_2/H_2S conditions, Corrosion Journal. ISSN: 0010-9312 69 (2) (February 2013) 145−156.

[12] NACE Publication 61114, Underdeposit Corrosion (UDC) Testing and Mitigation Methods in the Oil and Gas Industry, February 2014. NACE Item no. 24253.

[13] J.A.M. de Reus, E.L.J.A. Hendriksen, M.E. Wilms, Y.N. Al-Habsi, W.H. Durnie, M.A. Gough, Test methodologies and field verification of corrosion inhibitors to address under deposit corrosion in oil and gas production systems, Paper no. 05288, in: CORROSION/2005, NACE, Houston, TX, 2005.

[14] W.H. Durnie, M.A. Gough, J.A.M. de Reus, Development of corrosion inhibitors to address under deposit corrosion in oil and gas production systems, Paper no. 05290, in: CORROSION/2005, NACE, Houston, TX, 2005.

[15] J.H. Schön, Physical Properties of Rocks, Handbook of Petroleum Exploration and Production, Elsevier, 2011, ISBN 978-0-444-53796-6.

[16] J. Huang, Mechanistic Study of Under Deposit Corrosion of Mild Steel in Aqueous Carbon Dioxide Solution, Ohio University, 2013. Electronic Dissertation Retrieved from: https://etd.ohiolink.edu/.

[17] D. Rickard, G.W. Luther III, Chemistry of iron sulfides, Chemical Reviews 107 (2007) 514−562.

[18] C.I. Pearce, A.D. Pattrick, D.J. Vaughan, Electrical and magnetic properties of sulfides, Reviews in Mineralogy and Chemistry 61 (2006) 127−180.

[19] W.M. Telford, L.P. Geldart, R.E. Sheriff, Applied Geophysics, second ed., 1998, pp. 283−292.

[20] Y. Zheng, J. Ning, B. Brown, S. Nešić, Investigation of cathodic reaction mechanisms of H_2S corrosion using a passive SS304 rotating cylinder electrode, Corrosion Journal 72 (12) (2016) 1519−1525.

[21] P. Bai, Y. Liang, S. Zheng, C. Chen, Effect of amorphous FeS semiconductor on the corrosion behavior of pipe steel in H_2S-containing environments, I and EC Research: Industrial and Engineering Chemistry Research 55 (41) (2016) 10932−10940, http://dx.doi.org/10.1021/acs.iecr.6b03000.

[22] J. Ning, Y. Zheng, B. Brown, D. Young, S. Nesic, The role of iron sulfide polymorphism in localized H_2S corrosion of mild steel, Corrosion 73 (2) (2017) 155−168.

[23] Y. Zhang, J. Moloney, S. Mancuso, Understanding factors affecting corrosion inhibitor performance in under-deposit testing with sand, Paper no. 2575, in: CORROSION/2013, NACE, Houston, TX, 2013.

[24] J. Huang, B. Brown, S. Nesic, Localized corrosion of mild steel under silica deposits in inhibited CO_2 solutions, Paper no. 2144, in: CORROSION/2013, NACE, Houston, TX, 2013.

[25] B. Brown, A. Saleh, J. Moloney, Comparison of mono- to diphosphate ester ratio in inhibitor formulations for mitigation of under deposit corrosion, Corrosion Journal 71 (12) (December 2015) 1500−1510.

[26] Y. Zhang, J. Moloney, Electrochemical corrosion rate measurement under iron sulfide deposit, Corrosion Journal 72 (2016) 704.

[27] M. Achour, J. Kolts, P. Humble, R. Hudgins, Experimental evaluation of corrosion inhibitor performance in presence of iron sulfide in CO_2/H_2S environment, Paper no. 344, in: CORROSION/2008, NACE, Houston, TX, 2008.

[28] M.M. Salama, Influence of sand production on design and operations of piping systems, Paper no. 80, in: CORROSION/2000, NACE, Houston, TX, 2000.

[29] X. Landry, A. Runstedtler, S. Papvinasam, T. Place, Computational fluid dynamics study of solids deposition in heavy oil transmission pipeline, Corrosion Journal 68 (10) (October 2012) 904−913.

[30] A. Runstedtler, P. Boisvert, T. Place, Parametric modeling studies for sediment deposition as sites for under-deposit corrosion in oil transmission pipelines, Corrosion Journal 71 (6) (June 2015) 726−734.

[31] J.M. Dominguez Olivo, B. Brown, S. Nesic, Modeling corrosion mechanisms in the presence of quaternary ammonium chloride and imidazoline corrosion inhibitors, Paper no. C2016−7406, in: CORROSION/2016, NACE, Houston, TX, 2016.

[32] J. Moloney, W. Mok, C. Menendez, In situ assessment of pitting corrosion and its inhibition using a localized corrosion monitoring technique, Corrosion Journal 66 (2010) 065003-1−065003-18.

[33] W.M. Bohon, D.J. Blumer, A.F. Chan, K.T. Ly. NACE 1998, Paper 00073.

[34] D.I. Horsup, T.S. Dunstan, J.H. Clint, A break-through corrosion inhibitor technology for heavily fouled systems, Paper no. 07690, in: CORROSION/2007, NACE, Houston, TX, 2007.

[35] J.L. Crolet, Mechanisms of uniform corrosion under corrosion deposits, Journal of Material Science 28 (1993) 2589−2606.